A New Dry Tray Pressure Drop Model of Float Valve Trays

Jun Wang, Yi-Xuan Tang, Yan-Sheng Liu, Rui Cao, Tian-Xin Chen, Yu-Feng Hu, and Xue-Jun Fan
State Key Laboratory of Heavy Oil Processing, College of Chemical Engineering, China University of Petroleum, Beijing 102249, China

DOI 10.1002/aic.14027
Published online February 25, 2013 in Wiley Online Library (wileyonlinelibrary.com)

An accurate prediction of the dry pressure drop is very important for consideration of valve trays and for calculations in distillation field. Therefore, in this article, a series of hydraulic experiments were first conducted to reveal that the intermediate state during the valve opening process is closely related to the dry tray pressure drop under great valve weight. Then, a rigorous force analysis was made to show that Euler number is related only to the valve's position at the balance points for a certain valve type. Third, a new model for prediction of the dry tray pressure drop—which considers for the first time the influence of the intermediate state—was developed and then simplified for the purpose of convenient utilizations. Finally, the new model and its simplified form were tested by comparisons with the experimental results. The agreements are good, with the mean deviations being <5%. © 2013 American Institute of Chemical Engineers *AIChE J*, 59: 2694–2705, 2013

Keywords: valve tray, dry tray pressure drop, opening process, physical model, valve weight

Introduction

Distillation is the workhorse in petroleum and/or chemistry industry at present and in future.[1] In distillation, the heat and mass transfer between the gas phase and liquid phase occurs in the trays. The float valve tray has been used widely because of its high tray efficiency, low pressure drop, and a large operation range. And gas distribution on the tray determines the operating performance, the efficiency of the gas–liquid mass transfer, and other hydraulic parameters. The tray pressure drop is the most important factor affecting the gas distribution, especially at lower pressures.[2] At the same time, the dry tray pressure drop is a significant constituent part of the total pressure drop. Not only the dry tray pressure drop can reflect the tray operating condition as well as performance, but also it is the cornerstone for calculation of other hydraulic parameters.[3,4] Therefore, an accurate prediction of the dry pressure drop is the key point in considering the valve tray and will improve the calculations in distillation field.

As shown in Figure 1, the float valve flow channel includes the valve orifice and the space between the valve plate and tray. The tray without valve plate is called sieve tray. To some extent, the fluid flow through the sieves is relatively simple and has been extensively inveastigated.[3,5–7] On the other hand, it is difficult to analyze the flow process through automatic valves due to the complexity of the flow field. Consequently, few efforts have been made to solve this problem.[8,9] To get a good approximation of this flow type, the float valve is usually simplified as a "radial diffusers." The interaction between the fluid and the float valve was explored by investigating the flow conditions of fluid flowing in the radial diffusers.

Correspondence concerning this article should be addressed to Y. S. Liu at wsuper@cup.edu.cn or Y. F. Hu at huyf3581@sina.com.

© 2013 American Institute of Chemical Engineers

The radial flow between the float valve and the tray plate is similar to the radial flow between two parallel plates, which can be viewed as the original flow pattern.[10] A lot of radial flow application technologies have been developed including film drying, nozzle-flapper valve, air bearing, and reciprocating compressor, and the distillation valve tray is an exception. More specifically, the operating principle of all types of automatic valves is similar regardless of the structural differences.[11] The representative investigations on radial flow were made by Hayashi et al.,[12] Wark and Foss,[10] Boswirth,[13–15] Ferreira et al.,[9,16] Price and Botros,[17] Gasche et al.,[18] Possamai et al.,[19] Tang and Chang,[20] and Pereira.[21] Besides, the more relevant investigations on the system of this study have been made by Wood,[22] Bolles,[23] Klein,[24] and Lockett.[25]

On the basis of the assumption that the distributions of gas velocity are uniform under the valve disks, Wood[22] analyzed the forces on the valve and then developed a model. The simulation results on the basis of this model are consistent with the experimental results. However, both the simulation and the experiments were conducted using only a single float valve, and the movement of the valve in a multi-valve system has not been studied yet. Bolles[23] proposed a model by assuming that the operation mode of the valve resembles that of the sieve tray. In this model, the pressure drop curve was divided into three sections, namely the valve closed section, the valve opening process, and the valve full open section. And the drag coefficient in each section was used to calculate the dry tray pressure drop. Klein[24] simplified the Bolles' model by considering that the pressure drop between the closed and open balance point was a constant. Moreover, Klein's model used the orifice velocity instead of the slot velocity at the closed balance point and, therefore, allowed us to calculate the dry tray pressure drop more conveniently (see Appendix A for more detailed information). Likewise, on the basis of the Bolles' model, Lockett[25]

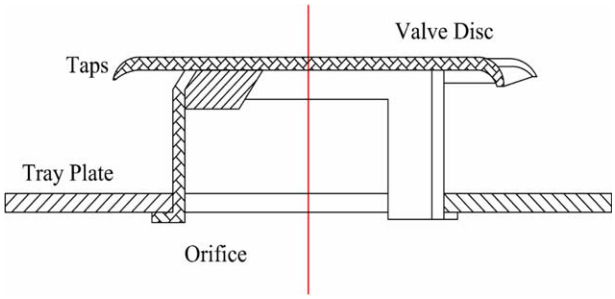

Figure 1. Schematic illustration of Glisch V-1 valve.

[Color figure can be viewed in the online issue, which is available at wileyonlinelibrary.com.]

introduced the pressure losses caused by the air flowing through the valve holes into the valve opening section. Although there are some other empirical dry tray pressure drop models,[26] it can be found that all these models[23–26] adopted the segmentation method. However, the corresponding force analysis on the float valve is simple, so much so that this empirical treatment has impaired the continuity of the pressure drop curve and has decreased the accuracy of the prediction for the gas flow velocity through the valve orifice at the balance point. In addition, these models ignore the influence of the intermediate state during valve opening process on the pressure drop, which was unacceptable in the case of a greater valve weight. Nevertheless, along with the increasing valve weight, the intermediate state played a more and more important role in affecting the variation tendency of pressure drop. This is discussed in more detail later.

In this work, an effort has been made for the first time to develop a model that can be used to predict the dry tray pressure drop over the whole valve opening process. In this new model, the influence of the intermediate state on the pressure drop was taken into account. We identified the presence of the inclined balance points by analyzing the data obtained using the large-scale experimental equipment that approaches the scale of the real commercial plant. Then, based on the detailed analysis of the forces acting on the valve, the correlations between the orifice gas velocity and

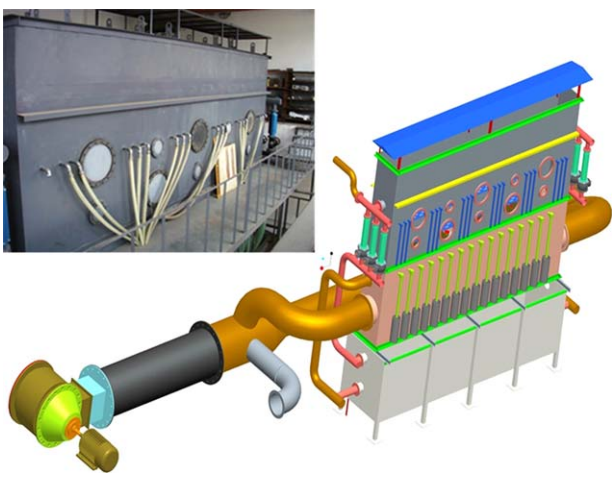

Figure 2. 3-D illustration of the experimental set-up (the insert is the photo of the experimental column).

[Color figure can be viewed in the online issue, which is available at wileyonlinelibrary.com.]

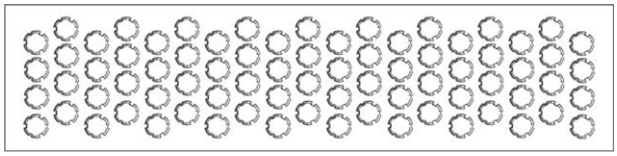

Figure 3. Configuration of the valves on one tray plate.

valve mass at the balance points were established. In addition, the new theoretical pressure drop model was simplified, so that it can be conveniently used in practical engineering work. The comparisons of the calculation results of our models are made both with the experimental results and with the results calculated using the previous models.[4,23]

Balance Points

Experimental part

As shown in Figure 2, the experimental equipment consists of three parts: the air supply system, the pressure measuring system, and the experimental column. The 6400 × 800 mm^2 experimental column is a rectangular column of double overflow, which is closer to the scale of the common industrial tower. The column is welded by carbon steel, with view-windows and manholes (made of plexiglass) on the wall for observation and for convenient installation of the tray. The column is equipped with three trays. The lowest tray is used to distribute uniformly the air from the air supply system and to collect the weeping. The middle tray is the test tray, and the upper one is used to gather the entrainment. There are four 1185 × 355 mm^2 valve tray plates on one side of the test tray, with 76 (19 × 4) float valves on the each plate (Figure 3 and Table 1). The tray pressure drop is measured by conventional U-shaped tube manometer. Each U-shaped tube manometer is connected to two pressure taps that are located above and below the test tray. Its schematic diagram is shown in Figure 4.

Using this equipment and Glisch V-1 float valve, we investigated the influences of gas velocity (in the 0–2.3 m/s range) and valve weight (32, 45, 58, and 80 g) on the dry tray pressure drop. The experimental conditions and the valve characteristics are shown in Tables 2 and 3. As shown in Figure 4, air passed from the blower through the gas control valve 8 and a flow-meter 6a. It was then divided into two lines. One of which went through the gas balance valve 7a, the flow-meter 6b, the right side of the gas distribution plate 3, the right side of the test tray 2, and finally into the atmosphere. The other passed progressively 7b, 6c, the left side, and finally into the atmosphere. Because the flow resistances in the two lines were different, when the gas control valve 8 was settled during the experiments, the gas balance valves 7a and 7b must be adjusted to maintain the equivalent gas flow in both branches. That is, the experimental results were recorded only when the U-shaped tube manometers on the lines 9c and 9e have given steady and unanimous liquid level difference.

Table 1. The Structure of the Cold Test Tray

Numbers of Valves on One Tray Plate	Numbers of Plates of One Side Flow Pass	Numbers of Flow Pass on the Test Tray	Total Numbers of Valves on the Test Tray
76	2 × 2	2	608

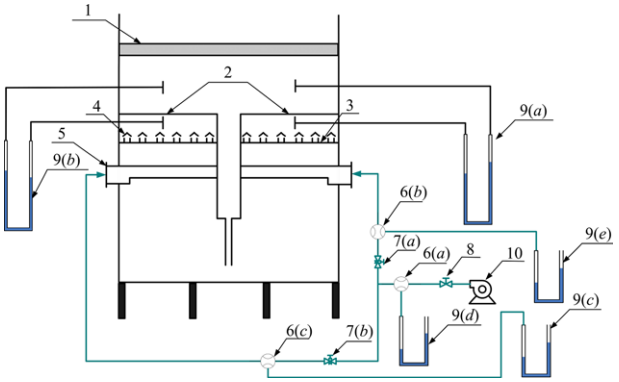

Figure 4. Schematic illustration of experimental column. 1, Gathering entrainment plate; 2, test valve tray; 3, gas distribution plate; 4, gas distributor; 5, air inlet pipe; 6a–6c, flow-meter; 7a and 7b, gas balance valve; 8, gas control valve; 9a–9e, U-shaped tube manometer; and 10, blower.

[Color figure can be viewed in the online issue, which is available at wileyonlinelibrary.com.]

Valves all inclined point and inclined balance point

Bolles[23] proposed the open and the closed balance points (cf. Figure A1 in Appendix A), with the assumption that the valve and the sieve trays have the same operation mode. The Bolles's valve opening model considers only the closed (Figure 7a) and the open states (Figure 7c). However, our experimental results clearly show that there also exist valves all inclined point and inclined balance point.

The dry tray pressure drop of heavy valve system as a function of gas velocity is shown in Figures 5 and 6. The step-increase in the pressure drop is observed for the first time, as the gas velocity increases. At first, the pressure drop progressively increases with the gas velocity, until the force of gas acting on the valve is equal to the gravity of the valve at the closed balance point A. And all the valves on the tray remain closed and are about to open at the special balance point A (Figure 7a). Then, one of the valves begins to open partly after the point A (in this study, this state is defined as the inclined state, see Figure 7b). Along with the continuous increase of the gas velocity, there are more and more inclined valves on the tray. At the inclined point B, all the valves are changed from closed state to inclined state. The valve will keep this inclined state in a small range of gas velocity, until it reaches the inclined balance point C where one of the valves was changed into fully open state (Figure 7c) whereas the rest remain unchanged. As the gas velocity continuously increases, all the valves become fully open (parallel state) in the open balance point D. In other words, the valves change from inclined state to full open in the course between point C and point D.

More experimental data associated with the inclined state of Glisch V-1 float valves are demonstrated in Figure 6.

Table 2. Experimental Conditions

Percentage of Open Area, η (%)	Experimental Medium	Superficial Velocity (m/s)	Temperature (°C)	Pressure (kPa)
14	Air	0–2.3	25	101.325

Table 3. Valve Characteristics

	Valve Diameter (m)	Orifice Diameter (m)	Valve Weight (g)	h_{max}[a] (m)	h_{min}[a] (m)
Glisch V-1	0.048	0.039	32; 45; 58; 80	0.009	0.0025

[*] h_{max} is the maximum valve height above the tray and h_{min} is the minimum valve height above the tray.

Once the valve weight exceeds 32 g, a clear pressure drop gradient, namely the valves all inclined point and the inclined balance point, will be observed between the closed and the open balance points. However, none of the valve theories/models available in the literature has considered the relationship between the pressure drop and the weighted valve behavior.

Theoretical Analysis and Modeling

Analysis of the forces acting on the float valve

The forces acting on the valve at the open balance point were analyzed at first. When the valve disk and the tray plate are parallel, the valve is subjected to the gravity, gas impact force, buoyancy, static pressure above/under the valve, and the support force. Buoyancy can be ignored, because the volume of the valve is small. The gas compressibility can also be ignored when Mach number (Ma) is <0.3. The specific force analysis is shown in Figure 8. In this analysis, F_t is the support force. F_o and F_u are the static pressures above and under the valve, respectively. mg is the gravity and F_i is the gas impact force. The dash line in the middle is the central axis, which is also the symmetry axis of orifice and disk (radius $r=0$). D is the disk diameter and d is the orifice diameter. The gas flow lateral area (A) obeys $A_d=\pi dh$ and $A_D=\pi Dh$.

Let P_0 be the static pressure above the valve equaling the atmosphere pressure. Let P_1, P_2, and P_3 denote the pressure after the contraction when the gas passes through the lateral area A_d, the pressure around the orifice edge, and the pressure of the disk edge, respectively. Then, Eq. 1 can be obtained, when the float valve is stable

$$mg+F_o=F_u+F_i+F_t \tag{1}$$

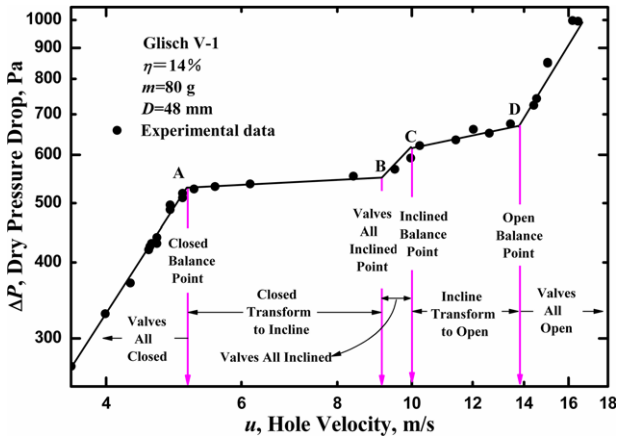

Figure 5. The dry pressure drop profile of heavy valve tray.

[Color figure can be viewed in the online issue, which is available at wileyonlinelibrary.com.]

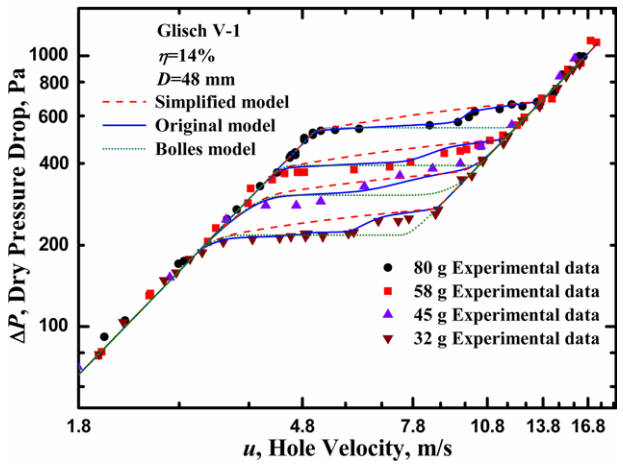

Figure 6. Comparisons of the experimental results with the results calculated by the original model, the simplified model, and Bolles model.

[Color figure can be viewed in the online issue, which is available at wileyonlinelibrary.com.]

with

$$F_o = 2\pi \int_0^{D/2} P_0 r dr \tag{2}$$

and

$$F_u = 2\pi \int_0^{d/2} P r dr + 2\pi \int_{d/2}^{D/2} P' r dr \tag{3}$$

Pressure Distribution in the Radial Range [0, d/2).. In the position of $r=d/2$, the gas was contracted suddenly. Consequently, the pressure was decreased from P_2 to P_1, and the gas velocity was increased rapidly. In the position of $r=D/2$, the eddy current appeared due to the taps on the disk and, therefore, the pressure was further decreased. An application of the orifice coefficient equation on A_d surface gives

$$\frac{\dot{m}}{\pi dh} = C_{D1}(2\rho_v \Delta P_1)^{0.5} \tag{4}$$

where C_{D1} is the orifice coefficient. $\dot{m}$ is the mass velocity of the gas flowing through the valve orifice. $\dot{m}$ is a function of the velocity of the gas (u) flowing through the orifice, gas density (ρ_v), and the orifice area ($\pi d^2/4$). That is

$$\dot{m} = 0.25\pi\rho_v u d^2 \tag{5}$$

Equation 4 can be rewritten as

$$\dot{m} \times \frac{\dot{m}}{\pi dh} = \frac{2\Delta P_1}{1/C_{D1}^2 \rho_v \pi dh} \tag{6}$$

The left-hand side of Eq. 6 describes the fluid's momentum-transfer rate. ΔP_1 is the driving force of momentum

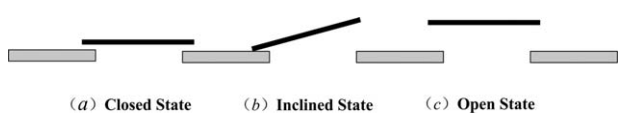

Figure 7. Valve opening steps: (*a*) closed state; (*b*) inclined state; and (*c*) open state.

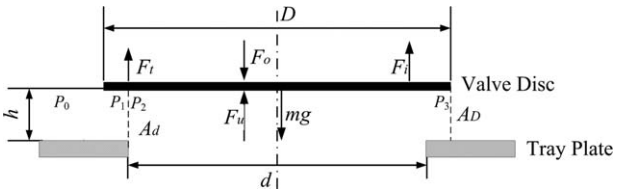

Figure 8. The forces acting on the valve when the valve disk and the tray plate are parallel.

transfer, and the denominator $1/C_{D1}^2\rho_v\pi dh$ represents the resistance of momentum transfer. Similarly, we can obtain

$$\dot{m} \times \frac{\dot{m}}{\pi Dh} = \frac{2\Delta P_2}{1/C_{D2}^2 \rho_v \pi Dh} \tag{7}$$

where C_{D2} is the orifice coefficient. The combination of the Componendo method with Eqs. 6 and 7 yields

$$\dot{m}^2 = \frac{2\rho_v(\Delta P_1 + \Delta P_2)}{\frac{1}{C_{D1}^2(\pi dh)^2} + \frac{1}{C_{D2}^2(\pi Dh)^2}} \tag{8}$$

Substitution of Eq. 5 into Eq. 8 yields

$$\frac{\rho_v \pi^2 u^2 d^4}{16} = \frac{2(\Delta P_1 + \Delta P_2)}{\frac{1}{C_{D1}^2(\pi dh)^2} + \frac{1}{C_{D2}^2(\pi Dh)^2}} \tag{9}$$

Equation 9 can be rewritten as

$$\Delta P_1 + \Delta P_2 = \frac{\rho_v u^2}{2}\left[\frac{1}{16C_{D1}^2}\left(\frac{d}{h}\right)^2 + \frac{1}{16C_{D2}^2}\left(\frac{d}{D}\right)^2\left(\frac{d}{h}\right)^2\right] \tag{10}$$

With the help of Bernoulli's theorem (the gravity of gas is neglected) for the region A_d and the cross section of the tray plate, we obtain

$$P_2 + \frac{1}{2}\rho_v\left(\frac{\dot{m}}{\rho_v \pi dh}\right)^2 = P_0 + \frac{1}{2}\rho_v u_s^2 + \Delta P_1 + \Delta P_2 \tag{11}$$

The velocity of the gas flowing through A_d is much larger than u_s and, therefore, Eq. 11 can be rewritten as

$$P_2 = \frac{\rho_v u^2}{32}\left(\frac{d}{h}\right)^2\left[\frac{1}{C_{D1}^2} + \frac{1}{C_{D2}^2}\left(\frac{d}{D}\right)^2 - 1\right] + P_0 \tag{12}$$

The results of Ferreira et al.[9] and Gasche et al.[18] showed that the pressure distribution is even under the valve in the radius range $[0, d/2)$. This suggests that the static pressure in $[0, d/2)$ equals P_2.

Pressure Distribution in the Radial Range (d/2, D/2).. Because of the short distance of the gas radial flow, the influence of the frictional resistance on pressure distribution can be neglected.[22] The pressure will decrease significantly, as the gas flows cross surface A_d. It follows from the Bernoulli's theorem for the region $d^- \sim d^+$ that

$$P_2 + \frac{1}{2}\rho_v\left(\frac{\dot{m}}{\rho_v \pi dh}\right)^2 = P_1 + \frac{1}{2}\rho_v\left(\frac{\dot{m}}{C_{D1}\rho_v \pi dh}\right)^2 + \Delta P_1 \tag{13}$$

where P_1 is the lowest pressure after the contraction when the gas passes through A_d. $\frac{1}{2}\rho_v\left(\frac{\dot{m}}{C_{D1}\rho_v\pi dh}\right)^2$ is the kinetic

pressure energy of the gas flow at the lowest pressure. Substitution of Eqs. 5, 6, and 12 into Eq. 13 gives the expression for the pressure in the position of $r=d^+/2$

$$P_1=\frac{\rho_v u^2}{32C_{D2}^2}\left(\frac{d}{h}\right)^2\left(\frac{d}{D}\right)^2-\frac{\rho_v u^2}{32C_{D1}^2}\left(\frac{d}{h}\right)^2+P_0 \tag{14}$$

Similarly, it follows from the Bernoulli's theorem for the region $D^- \sim D^+$ (both sides of suface A_D) that

$$P_3+\frac{1}{2}\rho_v\left(\frac{\dot{m}}{\rho_v \pi D h}\right)^2=P_0+\frac{1}{2}\rho_v u_s^2+\Delta P_2 \tag{15}$$

It is also evident that the velocity of gas flowing through A_D is much greater than u_s. This together with Eqs. 5, 7, and 15 yields the expression for the pressure in the position of $r=D^-/2$

$$P_3=\frac{\rho_v u^2}{32C_{D2}^2}\left(\frac{d}{D}\right)^2\left(\frac{d}{h}\right)^2-\frac{\rho_v u^2}{32}\left(\frac{d}{D}\right)^2\left(\frac{d}{h}\right)^2+P_0 \tag{16}$$

It is expected that the pressure is always proportional to the radius in the range of $(d/2, D/2)$. Therefore, the pressure P' at any radius r can be expressed as

$$P'=P_1+(r-d/2)\left(\frac{P_3-P_1}{D/2-d/2}\right) \tag{17}$$

Substitution of Eqs. 14 and 16 into Eq. 17 yields

$$\begin{aligned}P'=P_0&+\frac{\rho_v u^2}{32}\left(\frac{d}{h}\right)^2\left(\frac{2r-d}{D-d}\right)\left[\frac{1}{C_{D1}^2}-\left(\frac{d}{D}\right)^2\right]\\&+\frac{\rho_v u^2}{32C_{D2}^2}\left(\frac{d}{D}\right)^2\left(\frac{d}{h}\right)^2-\frac{\rho_v u^2}{32C_{D1}^2}\left(\frac{d}{h}\right)^2\end{aligned} \tag{18}$$

Substitution of Eqs. 12 and 18 into Eq. 3 provides the expression for the force caused by the static pressure under the valve

$$\begin{aligned}F_u=&\frac{\pi d^2}{4}\frac{\rho_v u^2}{32}\left(\frac{d}{h}\right)^2\left[\frac{1}{C_{D1}^2}+\frac{1}{C_{D2}^2}\left(\frac{d}{D}\right)^2-1\right]+\frac{\pi\rho_v u^2}{32}\left(\frac{d}{h}\right)^2\\&\left[\frac{1}{C_{D2}^2}\left(\frac{d}{D}\right)^2-\frac{1}{C_{D1}^2}\right]\left(\frac{D^2-d^2}{4}\right)+\frac{P_0\pi D^2}{4}\\&+\frac{\pi\rho_v u^2}{16(D-d)}\left(\frac{d}{h}\right)^2\left[\frac{1}{C_{D1}^2}-\left(\frac{d}{D}\right)^2\right]\left(\frac{D^3-d^3}{12}+\frac{d(d^2-D^2)}{8}\right)\end{aligned} \tag{19}$$

F_i can be calculated by[22]

$$F_i=\frac{1}{4}\pi d^2\rho_v u^2\sin\beta \tag{20}$$

with $\sin\beta=\frac{D-d/2^{0.5}}{\left[\left(D-d/2^{0.5}\right)^2+h^2\right]^{0.5}}$. Combination of Eqs. 1, 2, 19, and 20 gives (see Appendix II for more detailed information)

$$Eu=\frac{4k}{\pi D^2}\left(\frac{d}{h}\right)^2+2\left(\frac{d}{D}\right)^2\sin\beta \tag{21}$$

and

$$Eu=\Delta P_m/\left(\rho_v u^2/2\right) \tag{22}$$

The left-hand side of Eqs. 21 and 22 (i.e., Euler number, Eu) is the dimensionless variable. The conclusion, thus, obtained is that the Eu of float valves with the same structure is only a function of its position (h) at the balance points.

The above-mentioned force analysis suggests that the Eu at open/closed balance point satisfies Eq. 21. In the case of the asymmetric flow field of the inclined valve, however, it is difficult to carry out a force analysis of the float valve. For a convenient calculation, we assume that the Eu at any balance point (including the inclined state) always conforms to the above-mentioned conclusion. In real calculations, we can determine the expression for Eu by fitting to the gas velocity at the balance point for a given structure and, then, use this expression to provide various calculations for different valve weights (and the same structure).

Pressure drop model

Model Establishment. It is assumed that the float valve can have at most two states during the opening process, that is, the closed state and the inclined state or the inclined state and the open state. When the valve is at balance position, the flow equation of the fluid flowing through valves can be expressed as

$$\dot{m}^2=\frac{2\rho_v(\Delta P_1+\Delta P_2+\Delta P_3)}{\frac{1}{C_{D3}^2(\pi d^2/4)^2}+\frac{1}{C_{D1}^2(\pi dh)^2}+\frac{1}{C_{D2}^2(\pi Dh)^2}} \tag{23}$$

where C_{D3} is the orifice coefficient of the fluid flowing through the valve orifice. ΔP_1 is the pressure loss. The combination of Eqs. 5 and 23 gives

$$\Delta P=\Delta P_1+\Delta P_2+\Delta P_3=\frac{\rho_v u^2}{2C_{DS}^2} \tag{24}$$

with $\frac{1}{C_{DS}^2}=\left[\frac{1}{C_{D3}^2}+\frac{1}{16C_{D1}^2}\left(\frac{d}{h}\right)^2+\frac{1}{16C_{D2}^2}\left(\frac{d}{h}\right)^2\left(\frac{d}{D}\right)^2\right]$, where the value of C_{D3} is determined primarily by the orifice diameter, tray thickness, valve structure, and position.[20] Let C_{DC}, C_{DIn}, and C_{DO} denote the orifice coefficients at the closed, inclined, and open states, respectively. These orifice coefficients are constants, because the location of the valve is fixed. If the closed state and the inclined state coexist on the tray, then the mass balance equation is

$$N_1 u_I+(N-N_1)u_C=Nu \tag{25}$$

where N_1 is the number of the valves at the inclined state. N is the total number of the valves on the tray. u is the orifice velocity, and u_C is the gas velocity at the closed balance point. u_I is the gas velocity at the valves all inclined points. The balance equation of pressure drop is

$$\Delta P_f=\frac{1}{2}\rho_v\left(\frac{u_C}{C_{DC}}\right)^2=\frac{1}{2}\rho_v\left(\frac{u_I}{C_{DIn}}\right)^2 \tag{26}$$

Substitution of Eq. 26 into Eq. 25 yields

Table 4. Euler Number of Glisch V-1 Valve at Different Balance Points[a]

	Closed Balance Point	Valves All Inclined Point	Inclined Balance Point	Open Balance Point
Eu	28.69	8.24	7.47	3.96

[a]The parameters shown in this table were obtained by fitting to the experimental data of 80 g Glisch V-1 valve.

$$u_C = \frac{u}{\phi_I C_{DIn}/C_{DC} + 1 - \phi_I} \tag{27}$$

where ϕ_I ($=N_1/N$) stands for the number fraction of the inclined valves on the tray. It follows from Eq. 25 that

$$\phi_I = \frac{u - u_I}{u_I - u_C} \tag{28}$$

Substitution of Eq. 27 into Eq. 26 yields the expression for pressure drop

$$\Delta P_f = \frac{1}{2}\rho_v \left(\frac{u}{\phi_I C_{DIn} + (1-\phi_I) C_{DC}} \right)^2 \tag{29}$$

Similarly, if the inclined state and the open state coexist, then the mass balance equation is

$$N'_1 u_O + (N - N'_1) u_{IB} = Nu \tag{30}$$

where N'_1 is the number of the valves at the open state. u_O and u_{IB} are the gas velocity at the open balance point and the gas velocity at valves inclined balance point, respectively. $\phi_O (=N'_1/N)$ represents the number fraction of open valves on the tray. It can be obtained that

$$\Delta P_f = \frac{1}{2}\rho_v \left(\frac{u}{\phi_O C_{DO} + (1-\phi_O) C_{DIn}} \right)^2 \tag{31}$$

with

$$\phi_O = \frac{u - u_{IB}}{u_O - u_{IB}} \tag{32}$$

Equations 29 and 31 correspond to different valve states. The two equations are the same if $\phi_I = 1$ and $\phi_O = 0$. Therefore, this model is consecutive in the whole gas velocity range. It can also be observed that the apparent orifice coefficients are weighted average of those at the two adjacent balance states, and their respective weighting coefficients are the valves' number fraction of the corresponding state. In summary, Eqs. 28, 29, 31, and 32 are the equations of our original model that are used to calculate the dry tray pressure drop of float valve trays. If the influence of inclined state on dry tray pressure drop can be neglected, then the pressure drop model can be simplified as

$$\Delta P_f = \frac{1}{2}\rho_v \left(\frac{u}{\phi_O C_{DO} + (1-\phi_O) C_{DC}} \right)^2 \tag{33}$$

with

$$\phi_O = \frac{u - u_C}{u_O - u_C} \tag{34}$$

The orifice coefficients appeared in Eq. 33 are weighted average at the closed and the open states. The present model is more concise than the literature models.[23–26] It should be emphasized that the parameters involved in this simple model are the same as those involved in the literature models, which allows us to calculate the pressure drop in terms of the database available in the literature simply by setting $\phi_O \equiv 0$ (if $\phi_O < 0$), $\phi_O \equiv 1$ (if $\phi_O > 1$), and $0 \le \phi_O \le 1$.

Calculation Procedures. The calculation procedure is briefly described as follows.

1. Determine the *Eu* number at each balance point by fitting Eq. 22 to the experimental data and, then, calculate backward the gas velocity of orifice at all balance points using Eq. 22. For example, the *Eu* number for the Glisch V-1 valves was obtained from 80 g's data measured in this study, and the result is shown in Table 4. Then, the gas velocities corresponding to different valve weights (32, 45, and 58 g) were determined by using this *Eu* number, and the parameters are shown in Table 2. The results are shown in Table 5. Note that the simplified model requires only the *Eu* number at the closed and the open balance points.
2. Compute the valve number fraction of each state using Eq. 28 or 32 and Eq. 34 of the simplified model at any gas velocity in the experimental range.
3. Determine the orifice coefficient of valve at each state by regressing experimental data or using the existing database (the orifice coefficients determined from our data of 80 g Glisch V-1 valve for the closed, inclined, and open states are 0.169, 0.306, and 0.402, respectively).
4. Calculate the dry tray pressure drop using Eq. 29 or 31 and Eq. 33 of the simplified model (the typical calculation results are shown in Figure 6).

Results and Discussion

The influence of inclined state

The dry tray pressure drops of Glisch V-1 float trays with four valve weights are shown in Figure 6. The pressure drop gradient between the closed and the open balance points was observed clearly. And the heavier the valve is, the more evident the gradient will be. Obviously, the gradient stems from the transition of the valve state, and this result was never observed in the literature models. The possible reasons are as follows.

As shown in Table 4, the *Eu* numbers for the Glisch V-1 valve at valves all inclined and inclined balance points are 8.24 and 7.47, respectively. Therefore, the velocity of the gas through the valve orifice at these balance points can be expressed as

Table 5. Orifice Gas Velocity of Glisch V-1 with Different Weights at Different Balance Points

	Closed Balance Point	Valves All Inclined Point	Inclined Balance Point	Open Balance Point
80	5.09	9.49	9.97	13.69
58	4.33	8.08	8.49	11.66
45	3.82	7.12	7.47	10.27
32	3.22	6.00	6.31	8.66

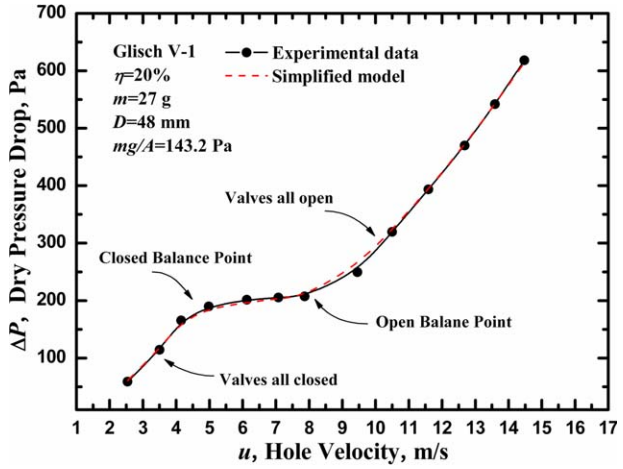

Figure 9. The typical pressure drop profile of light valve tray.

[Color figure can be viewed in the online issue, which is available at wileyonlinelibrary.com.]

$$u_{\mathrm{I}}=\left(\frac{8mg}{8.24\pi D^2\rho_{\mathrm{v}}}\right)^{0.5}\ \text{and}\ u_{\mathrm{IB}}=\left(\frac{8mg}{7.47\pi D^2\rho_{\mathrm{v}}}\right)^{0.5} \tag{35}$$

The pressure drops of the two balance points are obtained

$$\Delta P_{\mathrm{D}}=\frac{mg}{20\pi D^2 C_{\mathrm{DIn}}^2} \tag{36}$$

Equation 36 suggests that the pressure drop increases with increasing the valve weight. Indeed, Figure 6 shows that an increase in the valve weighs from 14 to 30 g promotes the pressure drop from 1.01 to 2.20 mm H_2O (i.e., from 9.91 to 21.57 Pa). It is also seen from Eq. 35 that $u_{\mathrm{I}} \approx u_{\mathrm{IB}}$. Therefore, the curve shown in Figure 9 for the pressure drop is usually smooth.[25]

To predict the orifice gas velocity at balance points, we proposed an analytic expression on the basis of the rigorous force analysis and identified the conditions under which the valve can reach the balance points. The calculated results for the gas velocities corresponding to various valve weights at the balance points through the valve orifice are shown in Table 5. It can be seen that the gas velocity at the balance points increases with increasing the valve weight.

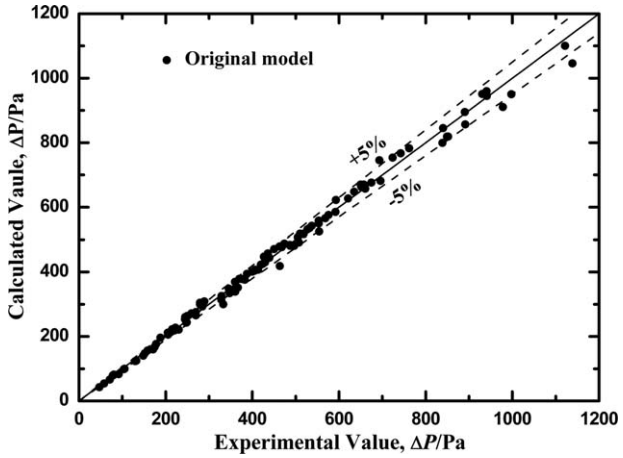

Figure 10. The deviation map of the original model.

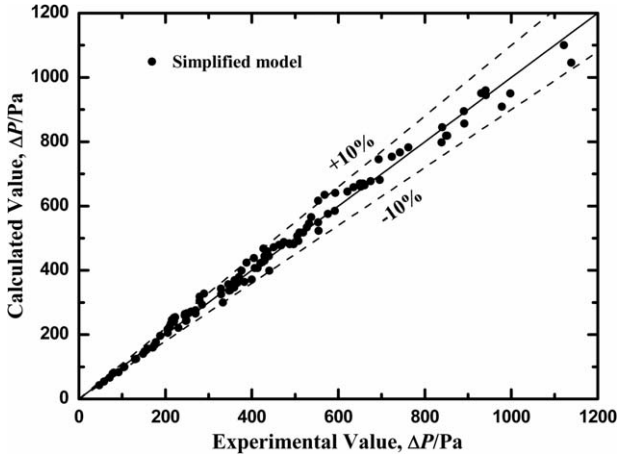

Figure 11. The deviation map of the simplified model.

The results calculated by the original pressure-drop model agree well with the experimental results. The deviation map of the original model is shown in Figure 10. The mean deviation is 3.08% (with the maximum absolute deviation being 9.70%). The deviation map of the simplified model is demonstrated in Figure 11, with the mean deviation and the maximum absolute deviation being 4.93 and 18.08%, respectively. Because the original model and the simplified one provided similar predictions for the pressure drop before the closed balance point or after the open balance point, the larger deviation of the simplified model is inevitably due to the neglect of the inclined state.

The significance of the intermediate state can also be confirmed by the Bolles model. As shown in Figure 6, the results calculated by the Bolles model agree well with the experimental values before the valves all inclined point, that is, in the case of the gas velocity $u<u_{\mathrm{I}}$. However, the calculated results are obviously smaller than the experimental values between the valves all inclined point and the open balance point. Furthermore, the Bolles model underestimates the gas velocity at the crucial open balance point. The deviation map of the Bolles model is presented in Figure 12, with mean deviation and the maximum positive (negative) deviation being 4.95 and 9.14% (−20.24%), respectively. These large deviations mean that the model calculations cannot be used in the tray design, the operating-condition estimation, and so forth.

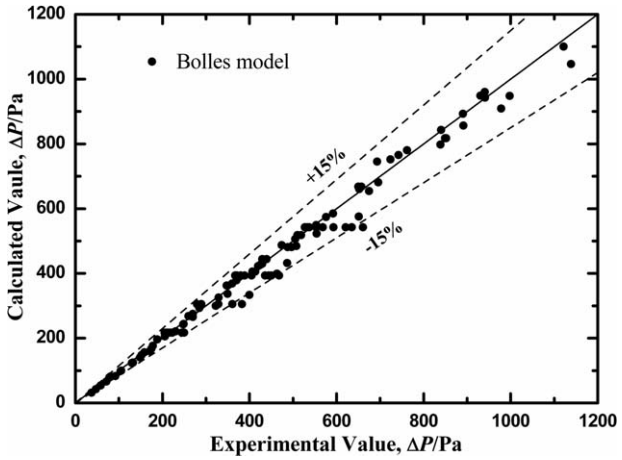

Figure 12. The deviation map of Bolles model.

The influence of the intermediate state on the tray pressure drop is investigated for the first time in this study. The model parameters of our original model and the simplified model are determined by fitting to the experimental data of the 80 g Glisch V-1 float valve. The results are shown in Figure 6. It can be found from Figures 6, 10, and 11 that the two models can provide accurate/acceptable predictions for the pressure drops. At the same time, the values calculated by the simplified model are greater both than those calculated by the original model and than the experimental values between the closed and open balance point. This phenomenon just demonstrates the existence of the inclined state in line with dissipation minimization, and it is this intermediate state that causes the dry pressure drop curve to be nearly horizontal with a light valve weight.

Model validation

The newly developed models were tested by comparisons with the reported experimental results and parameters and with the results calculated using the literature models.[4,23] Note that the experimental results shown in Figure A1 (cf. Appendix A) were reported without any parameter specification (e.g., the valve weight, etc.). Therefore, we back calculated the experimental valve weight using Eq. A5 (cf. Appendix A) and the calculated gas velocities.[23] The results are shown in Figure 13.

1. The gas velocities at the closed and the open balance points[4,23] were used in the calculations of the simplified model. The calculated results for the dry tray pressure drop are shown in Figures 13 and 14 and are denoted by simplified model*.
2. Glisch V-1 is a standard float valve. Therefore, the Glisch V-1 used in Ref. 23 should be the same as that used in the present measurements, and the gas velocities at all balance points were calculated using the present methods. The results for dry tray pressure drop are shown in Figure 13.

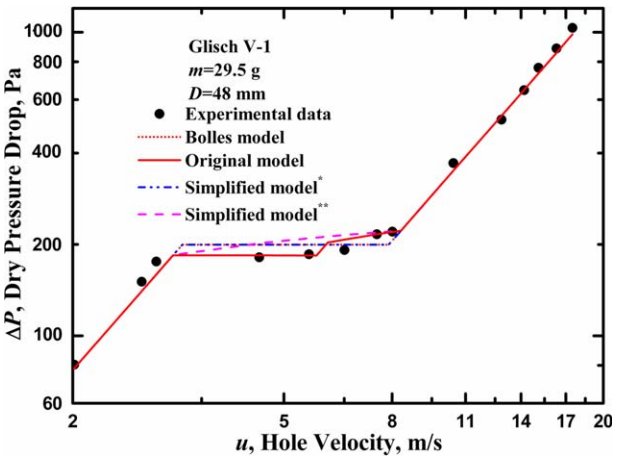

Figure 13. Comparisons of the experimental results[23] obtained using Glisch V-1 with the results calculated by the original model, the simplified model, and Bolles model.

***The model parameters are obtained from references 4 and 23. **The model parameters are calculated using the present method. [Color figure can be viewed in the online issue, which is available at wileyonlinelibrary.com.]**

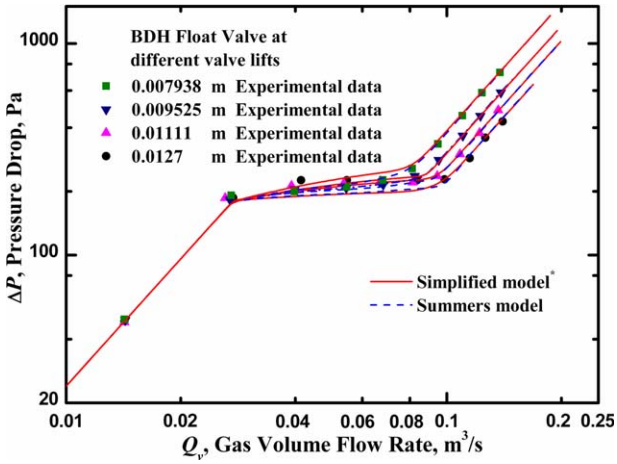

Figure 14. Comparisons of the calculation results of the simplified model with the experimental results[4] and with the results calculated by Summers model.

[Color figure can be viewed in the online issue, which is available at wileyonlinelibrary.com.]

The conclusions, thus, obtained from Figures 13 and 14 are as follows.

1. The profile of pressure calculated by the simplified model* is almost the same as that calculated by the Bolles model (Glisch V-1) or by the Summers model (BDH), confirming that the present models can be utilized to calculate accurately the dry pressure drop in terms of the available database for various kinds of valves.
2. The position of the closed/open balance point cannot be determined accurately owing to the large sampling intervals used in Ref. 23. However, the experimental results for the nearby points suggest that the pressure drops predicted by the Bolles model will show positive/negative deviations from the experimental results at the closed/the open balance points, respectively. These deviations will reflect themselves in the gas velocities predicted by the Bolles model at balance points.
3. The simplified model** yields more accurate results than the Bolles model for the pressure drop and the gas velocity at the closed/open balance point. However, its predictions are still greater than the experimental results due to the neglect of the effect of the intermediate state.
4. The pressure drops calculated by the original model agree well with the experimental results over the whole gas velocity range. The original model also yields more reasonable predictions for the gas velocities at balances points than the rest models examined herein.

Conclusions

The influence of the valve weight on the pressure drop has been investigated. The float valve undergoes progressively the closed, inclined, and open states, as the gas velocity increases. Accordingly, there appears four special balance points in the course of the valve opening process, that is, the closed balance point, the valves all inclined point, the inclined balance point, and the open balance point. Correspondingly, the whole opening process is divided into the closed zone, the closed-inclined zone, the valves all inclined

zone, the inclined-open zone, and the open zone. The inclined state thereof is an intermediate state and is closely related to the dry tray pressure drop under great valve weight.

An analytic equation has been proposed on the basis of a rigorous force analysis to predict the orifice gas velocity at balance points. The conditions under which the valve can reach the balance points have been identified. The Euler number at balance points is a constant for a given kind of valve. Moreover, the proposed equation is applicable to other kinds of float valves because of its theoretical basis.

A new model has been established for prediction of the dry tray pressure drop during the opening process. The parameters (the inclined and open fractions, ϕ_I and ϕ_O) are introduced into the model, so that the pressure drop can be predicted over the whole gas velocity range and the pressure drop can be directly associated with the average orifice gas velocity. The orifice coefficient involved in the model is the weighted average of the orifice coefficients at two adjacent states, and its weighting coefficients are the valves' number fraction of the float valves at different states.

The calculation results of the original model are in good agreement with our experimental results, whereas the simplified model thereof shows slightly larger deviations from the experimental results. However, we have calculated the pressure drops of the BDH float valve with different lifts using the simplified model and the parameters available in Ref. 4. The comparisons with the experimental results show that the accuracy of the prediction of the simplified model is comparable to the accuracy of the predictions of the literature models. Furthermore, the simplified model is simple in form. Therefore, the present models provide a convenient and accurate approach for calculation of the pressure drops of various kinds of float valves.

Acknowledgments

The authors gratefully acknowledge the assistance of Tao Chen, GuiZheng Li, and LeHuan Wu for conducting the preliminary experiments. This research was funded by the China National Petroleum Corporation (CNPC), the National Natural Science Foundation of China (21176248, 20976189, and 21076224), and Science Foundation of China University of Petroleum, Beijing (qzdx-2011-01).

Notation

A_d = gas flow lateral area between valve orifice and disk, m^2
A_D = gas flow lateral area between tray plate and valve disk, m^2
C_{D1} = orifice coefficient of the gas flowing through the A_d surface
C_{D2} = orifice coefficient of the gas flowing through the A_D surface
C_{D3} = orifice coefficient of the gas flowing through the valve orifice
C_{DC} = orifice coefficient of valve closed
C_{DIn} = orifice coefficient of valve inclined
C_{DO} = orifice coefficient of valve open
C_{DS} = apparent orifice coefficient
D = valve plate diameter, m
d = valve orifice diameter, m
Eu = Euler number
F_i = force due to the change of gas momentum, N
F_o = force due to static pressure above the valve plate, N
F_t = support force of the tray, N
F_u = force due to static pressure below the valve plate, N
g = gravity acceleration, m/s^2
h = height between the valve disk and the tray, m
k = model parameter
Ma = Mach number
m = valve mass, kg
$\dot{m}$ = gas flow rate in mass, kg/s
P_0 = static pressure above the valve equaling the atmosphere pressure, Pa
P_1 = pressure after the contraction when the gas passes through the lateral area A_d, Pa
P_2 = pressure around the orifice edge, Pa
P_3 = pressure around the disk edge, Pa
ΔP_1 = pressure drop due to the gas flowing through the A_d face, Pa
ΔP_2 = pressure drop due to the gas flowing through the A_D face, Pa
ΔP_3 = pressure drop due to the gas flowing through the orifice, Pa
ΔP_f = total pressure drop, Pa
u = velocity of the gas flowing through the valve orifice
u_C = velocity of the gas flowing through the valve orifice at the closed balance point, m/s
u_{IB} = velocity of the gas flowing through the valve orifice at the inclined balance point, m/s
u_I = velocity of the gas flowing through the valve orifice at the valves all inclined balance point, m/s
u_O = velocity of the gas flowing through the valve orifice at the open balance point, m/s
u_s = superficial gas velocity, m/s

Greek letters

β = angle change value after gas flows through the valve, °
ϕ = valve's number fraction of inclined or open state on the tray
η = percentage of open area, %
ρ_v = gas density, kg/m^3

Literature Cited

1. Fair JR. The workhorse today and tomorrow—distillation. *Chem Eng (NY)*. 2002;109:108–110, 112.
2. Kister HZ, Olsson M. Understanding maldistribution in 3-pass trays. *Chem Eng Res Des*. 2011;89:1397–1404.
3. Summers DR. Dry tray pressure drop of sieve trays: a new correlation that matches most commercial trays. *Chem Eng (NY)*. 2009;116:36–39.
4. Summers DR, Van Sinderen A. Dry tray pressure drop of rectangular float valve and V-Grid trays. In: The Distillation Symposium. 2001 AIChE Spring National Meeting, Houston, Texas, 2001.
5. Smith PL, Van Winkle M. Discharge coefficients through perforated plates at Reynolds Numbers of 400 to 3000. *AIChE J*. 1958;4:266–268.
6. Stichlmair J, Mersmann A. Dimensioning plate columns for absorption and rectification. *Int Chem Eng*. 1978;18:223–236.
7. Cervenka J, Kolar V. Hydrodynamics of plate columns VIII—the dry plate pressure drop of sieve plate separating columns. *Collect Czech Chem C*. 1967;38:2891–2897.
8. Matos FFS, Prata AT, Deschamps CJ. Numerical analysis of the dynamic behavior of plate valves in reciprocating compressors. In: International Conference on Compressors and Theirs Systems, City University, London, 1999:453–462..
9. Ferreira RTS, Deschamps CJ, Prata AT. Pressure distribution along valve reeds of hermetic compressors. *Exp Therm Fluid Sci*. 1989;2:201–207.
10. Wark CE, Foss JF. Forces caused by the radial outflow between parallel disks. *J Fluid Eng*. 1984;106:292–297.
11. Touber S. A contribution to the improvement of compressor valve design. Ph.D. Thesis. The Netherlands: Delft University, 1976.
12. Hayashi S, Matsui T, Ito T. Study of flow and thrust in nozzle-flapper valves. *J Fluid Eng*. 1975;97:39–50.
13. Boswirth L. Theoretical and experimental study on fluid flow in valve channels, part I and II. In: The International Compressor Engineering Conference at Purdue University, West Lafayette, USA. 1982:38–53.
14. Boswirth L. A model for valve flow taking non-steady flow into account. In: The International Compressor Engineering Conference at Purdue University, West Lafayette, USA. 1984:227–241.
15. Boswirth L. Valve flow experiments with enlarged models. In: The International Compressor Engineering Conference at Purdue University, West Lafayette, USA. 1986:28–54.
16. Ferreira TS, Lainor L. Analysis of the influence of valve geometric parameters on the effective flow and force areas. In: The International Compressor Engineering Conference at Purdue University, West Lafayette, USA. 1986:632–646.
17. Price GR, Botros KK. Numerical and experimental analysis of the flow characteristics through a channel valve. In: The International

Compressor Engineering Conference at Purdue University, West Lafayette, USA. 1992:1215–1225.
18. Gasche JL, Ferreira RTS, Prata AT. Pressure distributions along eccentric circular valve reeds of hermetic compressors. In: The International Compressor Engineering Conference at Purdue University, West Lafayette, USA. 1992:1189–1198.
19. Possamai FC, Ferreira RTS, Prata AT. Pressure distribution in laminar radial flow through inclined disks. *Int J Heat Fluid Flow*. 2001;22:440–448.
20. Tang C, Chang Y. Computational and experiment study of the orifice discharge coefficient influenced by the presence of a rigid plate. *Prog Comput Fluid Dyn*. 2007;7:439–446.
21. Pereira ELL, Deschamps CJ. A theoretical account of the piston influence on effective flow and force areas of reciprocating compressor valves. In: The International Compressor Engineering Conference at Purdue University, West Lafayette, USA. 2010:No.1359.
22. Wood RM. The stability of the valves of floating valve plates. *Trans Inst Chem Eng*. 1961;39:313–317.
23. Bolles WL. Estimating valve tray performance. *Chem Eng Prog*. 1976;72:43–47.
24. Klein GF. Simplified model calculates valve–tray pressure drop. *Chem Eng (NY)*. 1982;89:81–85.
25. Lockett MJ. Distillation tray fundamentals. London: Cambridge University Press, 1986:82–86.
26. Piqueur H, Verhoeye L. Research on valve trays hydraulic performance in the air–water system. *Can J Chem Eng*. 1976;54:177–184.

Appendix A

A Brief Introduction of Bolles Model

Bolles proposed a valve-sieve tray analogy approach and established a model for valve trays that differs from sieve trays in slot area and in drag coefficient. The behavior of valves was described in Bolles model at various gas velocities:

- At relatively high vapor loads, all valves are fully open and pressing against their upper stops. Under these conditions the slot area is a constant, and the valve tray behaves like a sieve tray of high hole area.
- At relatively low vapor loads, all valves are closed and pressing against their lower stops, which are usually set for a small residual open clearance. Under these conditions, the slot area is also a constant, and the valve tray behaves like a sieve tray of low hole area.
- At certain intermediate loads, some of valves are fully open, whereas others closed. The dynamic characteristics of the valves are such that, at most of the times, each individual valve is either fully open or fully closed. That is, no valve remains stable in an intermediate position of travel.

Open and closed balance points

As shown in Figure A1, the point at which all valves are open and the first valve starts to close is called the "open balance point." The condition existing when all valves are closed and the first valve starts to open is called the "closed balance point."

Establishment of model

When a valve is open, the valve unit may be treated as a pipe fitting and the pressure loss can be expressed in terms of kinetic energy

$$\Delta P = \frac{1}{2} K_{\mathrm{vo}} \rho_{\mathrm{v}} u_{\mathrm{vh}} \tag{A1}$$

where ΔP is the pressure loss through valve unit. u_{vh} is the velocity of vapor through hole. K_{vo} is the coefficient for pressure loss, valve open, based on hole area. ρ_{v} is the density of vapor. Similarly, when a valve is closed the pressure loss may be expressed as

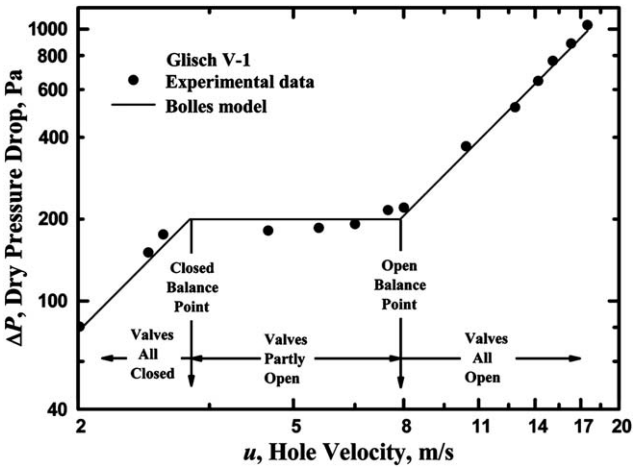

Figure A1. The open and the closed balance points.[23]

$$\Delta P = \frac{1}{2} K'_{vc} \rho_{\mathrm{v}} u_{\mathrm{vsc}}^2 \tag{A2}$$

where u_{vsc} is the velocity of vapor through slot area, valve closed. K'_{vc} is the coefficient for pressure loss, valve closed, based on slot area.

When a valve is partially open, the major source of dry pressure drop is the weight of the valve, which is supported by pressure on the underside of the valve. The weight of the valve (m_{v}) is given by

$$m_{\mathrm{v}} = \mathrm{A}_{\mathrm{v}} H_{\mathrm{v}} \rho_{\mathrm{vm}} R_{\mathrm{vw}} \tag{A3}$$

where R_{vw} is the ratio of the weight of the whole valve with legs to the weight of the valve lid without legs. A_{v} is the area of the latter valve. H_{v} is the thickness of the valve. ρ_{vm} is the density of valve metal. The pressure drop is given by

$$\Delta P = C_{\mathrm{vm}} H_{\mathrm{v}} R_{\mathrm{vw}} \rho_{\mathrm{vm}} g \tag{A4}$$

where the coefficient C_{vm} is introduced to account for eddy losses. The values of the valve coefficients (K_{vo}, K'_{vc}, and C_{vm}) are determined from the experimental data on the flow of vapor through a dry valve tray.

The open balance point, based on hole area (A_{h}), corresponds to the simultaneous solution of Eqs. A1 and A4 for the elimination of ΔP, which results in

$$u_{\mathrm{vhob}} = [2 g H_{\mathrm{v}} R_{\mathrm{vw}} (C_{\mathrm{vm}} / K_{\mathrm{vo}}) (\rho_{\mathrm{vm}} / \rho_{\mathrm{v}})]^{0.5} \tag{A5}$$

Similarly, the closed balance point, based on slot area (A_{sc}; valve closed), corresponds to the simultaneous solution of Eqs. A2 and A4

$$u_{\mathrm{vscb}} = [2 g H_{\mathrm{v}} R_{\mathrm{vw}} (C_{\mathrm{vm}} / K'_{\mathrm{vc}}) (\rho_{\mathrm{vm}} / \rho_{\mathrm{v}})]^{0.5} \tag{A6}$$

where u_{vhob} is the velocity of vapor through holes, open balance point. u_{vscb} is the velocity of vapor through slot area, closed balance point.

The ratio (proportion) of valve open (υ_{o}) is obtained by invoking a mass balance on vapor passing through the open and the closed valves

$$Q_v = \upsilon_o A_h u_{vhob} + (1-\upsilon_o) A_{sc} u_{vscb} \quad \text{(A7)}$$

Because the mean hole velocity is defined by

$$u_{vh} = Q_v / A_h \quad \text{(A8)}$$

the expression for Q_v can be obtained from Eq. A8 and, then, can be substituted into Eq. A7 to yield

$$A_h u_{vh} = \upsilon_o A_h u_{vhob} + (1-\upsilon_o) A_{sc} u_{vscb} \quad \text{(A9)}$$

That is

$$\upsilon_o = \left(u_{vh} - \frac{A_{sc}}{A_h} u_{vscb}\right) / \left(u_{vhob} - \frac{A_{sc}}{A_h} u_{vscb}\right) \quad \text{(A10)}$$

Calculation procedures

In practice, Eqs. A5 and A6 are used to compute the vapor velocity at the open and closed balance points. Equation A10 is used to compute the ratio of valves open. Finally, the dry tray drop is computed by Eqs. A1, A2, or A4 according to the value of υ_o.

A Brief Introduction of Klein Model

Klein used Bolles model with some simplification for the dry tray pressure drop calculation. More specifically, Klein used the hole velocity rather than the slot velocity in Bolles model at the valve closed state and expressed the pressure loss in terms of kinetic energy

$$\Delta P = K_c \rho_v u_{vh}^2 \quad \text{(A11)}$$

Similarly, the loss when a valve is fully open can be expressed as

$$\Delta P = K_o \rho_v u_{vh}^2 \quad \text{(A12)}$$

where K_o and K_c are valve coefficients in Klein model. The hole velocity in Klein model at the closed balance point (u_{vhcb}) and at open balance point (u_{vhob}) is expressed as

$$u_{vhcb} = [g H_v R_{vw} (C_{vm}/K_c)(\rho_{vm}/\rho_v)]^{0.5} \quad \text{(A13)}$$

and

$$u_{vhob} = [g H_v R_{vw} (C_{vm}/K_o)(\rho_{vm}/\rho_v)]^{0.5} \quad \text{(A14)}$$

with

$$\frac{u_{vhcb}}{u_{vhob}} = \left(\frac{K_o}{K_c}\right)^{0.5} \quad \text{(A15)}$$

where C_{vm} is eddy losses coefficient in the Klein model. Between u_{vhcb} and u_{vhob}, the pressure drop remains unchanged despite of the increase in the hole velocity. The valves oscillate between the closed and the open balance positions and are not stable in an intermediate position. In Klein's opinion, the change in slot area can compensate the velocity's augment owing to this valve oscillation. Therefore, the gas flowing through the slot area in a relatively steady velocity does not result in any change in pressure drop.

Calculation procedure

When $u_{vh} < u_{vhcb}$, the dry tray pressure drop is calculated by Eq. A11. Equation A12 can be used if $u_{vh} > u_{vhob}$. When a tray operates between u_{vhcb} and u_{vhob}, because the pressure drop is a constant, Klein used a horizontal line in place of the equation developed by Bolles. Therefore, the ratio of valves open, υ_o, is not required in Klein model. As long as the u_{vhcb} (or u_{vhob}) is calculated using Eq. A13 (or Eq. A14), the dry tray pressure drop can be obtained either by Eq. A11 or by Eq. A12 in this intermediate range.

Note that in the Bolles model the slot velocity and the coefficient for pressure loss are calculated using the slot area at valve closed state. The slot area can be obtained from the valve tray proprietor or from the experimental measurements of an actual valve. When computing the slot area, the portions of the slot obstructed by legs or dimples must be subtracted. However, the slot area is sometimes unknown, and the corresponding calculations may be unwieldy, especially for an operating column. On the other hand, the hole area is generally known (e.g., Standards) and is more widely used by engineers. Therefore, the replacements of the slot area and the slot velocity by the hole area and the orifice velocity allow the Klein model to calculate pressure drop more conveniently.

Appendix B

Combination of Eqs. 1, 2, 19, and 20 gives the expression for the forces acting on the valve, when the valve disk and the tray are parallel

$$mg = \frac{\pi d^2}{4}\frac{\rho_v u^2}{32}\left(\frac{d}{h}\right)^2\left[\frac{1}{C_{D1}^2} + \frac{1}{C_{D2}^2}\left(\frac{d}{D}\right)^2 - 1\right] + \frac{\pi d^2}{4}\rho_v u^2 \sin\beta + \frac{\pi \rho_v u^2}{16(D-d)}\left(\frac{d}{h}\right)^2\left[\frac{1}{C_{D1}^2} - \left(\frac{d}{D}\right)^2\right]\left[\frac{D^3-d^3}{12} + \frac{d(d^2-D^2)}{8}\right] + \frac{\pi \rho_v u^2}{32}\left(\frac{d}{h}\right)^2\left[\frac{1}{C_{D2}^2}\left(\frac{d}{D}\right)^2 - \frac{1}{C_{D1}^2}\right]\left(\frac{D^2-d^2}{4}\right) + F_t \quad \text{(B1)}$$

If the valve is at the open or closed balance point, then the support force can be neglected. Therefore, Eq. B1 can be simplified as

$$mg = \frac{\pi d^2}{4}\frac{\rho_v u^2}{32}\left(\frac{d}{h}\right)^2\left[\frac{1}{C_{D1}^2} + \frac{1}{C_{D2}^2}\left(\frac{d}{D}\right)^2 - 1\right] + \frac{\pi d^2}{4}\rho_v u^2 \sin\beta + \frac{\pi \rho_v u^2}{16(D-d)}\left(\frac{d}{h}\right)^2\left[\frac{1}{C_{D1}^2} - \left(\frac{d}{D}\right)^2\right]\left[\frac{D^3-d^3}{12} + \frac{d(d^2-D^2)}{8}\right] + \frac{\pi \rho_v u^2}{32}\left(\frac{d}{h}\right)^2\left[\frac{1}{C_{D2}^2}\left(\frac{d}{D}\right)^2 - \frac{1}{C_{D1}^2}\right]\left(\frac{D^2-d^2}{4}\right) \quad \text{(B2)}$$

Equation B2 shows that the gas velocity at balance points is related to the valve mass (m), valve position (h), and structural parameters such as d, D, C_{D1}, C_{D2}, and so forth.

Parameter Analysis

C_{D1} is the orifice coefficient of the gas crossing the A_d surface. If the A_d plane is viewed as a channel, then its thickness is $\Delta d = d^+/2 - d^-/2$ with $\Delta d \to 0$. And, its orifice coefficient is $\sim$0.611 (the influence of Reynolds number is neglected). C_{D2} is the orifice coefficient of the gas crossing the A_D surface. First, if taps or legs do not exist at the valve edge, then the local resistance loss of the gas crossing A_D surface can be attributed to the sudden expansion flow (the influence of Reynolds number is neglected). Under this condition, the value of the coefficient of local resistance is 1, as the tray area is much larger than the valve slot area.

However, the presence of taps and legs can lead to the eddy losses and other effects at the valve edge. The valve disk above the orifice will also change the direction of the gas flow. If we use ξ (coefficient of local resistance) to represent the influences of these factors, then we obtain the relationship $C_{D2} = 1/(1+\xi)^{0.5}$, with $1+\xi$ being the overall resistance coefficient of valve at A_D. It is evident that C_{D2} is a function of valve structure and position (h), which depends on the specific circumstance. Let $A = \left[\frac{1}{C_{D1}^2} + \frac{1}{C_{D2}^2}\left(\frac{d}{D}\right)^2 - 1\right]$, $B = \left[\frac{1}{C_{D1}^2} - \left(\frac{d}{D}\right)^2\right]$, and $C = \left[\frac{1}{C_{D2}^2}\left(\frac{d}{D}\right)^2 - \frac{1}{C_{D1}^2}\right]$, then Eq. B2 can be rewritten as

$$\frac{mg}{\rho_v u^2/2} = \left(\frac{d}{h}\right)^2 \left\{\frac{A\pi d^2}{64} + \frac{B\pi}{8(D-d)} \left[\frac{D^3-d^3}{12} + \frac{d(d^2-D^2)}{8}\right] + \frac{C\pi}{16}\left(\frac{D^2-d^2}{4}\right)\right\} + \frac{\pi d^2}{2}\rho_v u^2 \sin\beta \tag{B3}$$

That is

$$\frac{4mg/\pi D^2}{\rho_v u^2/2} = \left(\frac{d}{h}\right)^2 \frac{4k}{\pi D^2} + 2\left(\frac{d}{D}\right)^2 \sin\beta \tag{B4}$$

with $k = \frac{\pi D^2}{4}\left\{\frac{A}{16}\left(\frac{d}{D}\right)^2 + \frac{B}{8}\left[\frac{1}{3} - \frac{1}{6}\left(\frac{d}{D}\right) - \frac{1}{6}\left(\frac{d}{D}\right)^2\right] + \frac{C}{16}\left(1 - \left(\frac{d}{D}\right)^2\right)\right\}$. It follows from $\Delta P_m = 4mg/\pi D^2$ and Eq. B4 that

$$Eu = \frac{4k}{\pi D^2}\left(\frac{d}{h}\right)^2 + 2\left(\frac{d}{D}\right)^2 \sin\beta \tag{B5}$$

and

$$Eu = \Delta P_m / \left(\rho_v u^2/2\right) \tag{B6}$$

where k is an equation parameter and is a function of valve structure and position (h).

Manuscript received July 2, 2012, and revision received Dec. 23, 2012.